Journal of Applied Electrochemistry (2006) 36:1157–1162
DOI 10.1007/s10800-006-9200-5

Magneto-sensitive nickel nanowires fabricated by electrodeposition into multi- and single-ion track templates

T. OHGAI[1,4,*], I. ENCULESCU[1,5], C. ZET[1], L. WESTERBERG[2], K. HJORT[3], R. SPOHR[1,3] and R. NEUMANN[1]
[1]*Materials Research Department, Gesellschaft für Schwerionenforschung (GSI), D-64291, Darmstadt, Germany*
[2]*The Svedberg Laboratory, Uppsala University, Box 533, S-75121, Uppsala, Sweden*
[3]*The Angstrom Laboratory, Uppsala University, Box 534, S-75120, Uppsala, Sweden*
[4]*Faculty of Engineering, Nagasaki University, Nagasaki, 852-8521, Japan*
[5]*National Institute of Materials Physics, 76900, Bucharest, Romania*
*(*author for correspondence, tel.: +81-95-819-2638, fax: +81-95-819-2638, e-mail: ohgai@nagasaki-u.ac.jp)*

Received 3 April 2006; accepted in revised form 30 June 2006

Key words: electrodeposition, ion beam, magnetoresistance, nanochannel, nickel, polycarbonate

Abstract

Polycarbonate templates of (30 ± 1) μm thickness containing cylindrical etched-track nanochannels of (500 ± 50) nm diameter were used for electrodeposition of Ni nanowires. Using 10^4 channels per cm^2, the most favourable deposition potential of -1.0 V was determined in a potentiostatic mode by varying the deposition potential with respect to an Ag/AgCl reference electrode over a range between -0.1 V and -1.5 V. The deposition efficiency at -1.0 V was estimated around 10%. The resulting single wires had a resistance around 200 Ω and showed an anisotropic magnetoresistance (AMR) effect of 1%, applicable to directionally sensitive magnetic field sensors.

1. Introduction

Recently, novel fabrication techniques of nanowires [1, 2] have received much attention due to an increasing interest in wires close to or below the critical size limit for quantum effects. So far, commercially available etched ion-track membranes of polycarbonate [3–5] or anodized aluminum oxide films [6–8] with high area density of nanochannels (about 10^8–10^{10} channels cm^{-2}) [9–11] have been used as templates. In many commercial templates, the incidence angles of the nanochannels scatter within a certain range. Furthermore, the channels can be conical-shaped or have the shape of a toothpick, which is far from cylindrical. For nanofabrication it would be advantageous if the channel position, inter-channel distance, and channel diameter and shape could be controlled precisely [12, 13]. Lithographic Galvanoforming (LIGA) techniques based on X-rays, have been applied to fabricate novel electronic devices. Using a similar heavy-ion LIGA technique [14–18], metallic nanowires with much higher aspect ratio can be synthesized, however, presently still with random positioning. This has been demonstrated for polycarbonate and polyimide at nanochannel densities around 10^8 channels cm^{-2} [19].

In this study, a polycarbonate film was irradiated using energetic heavy-ion beams to form straight tracks perpendicular to the film. Subsequently, the films were selectively etched to create cylindrical nanochannels of high quality in terms of orientation, surface roughness, shape, and size distribution of the channels over a wide range of area density (from 1 pore per sample to 10^4 pores cm^{-2}), however, spatially distributed at random. The electrodeposition of nickel nanowires and their anisotropic magnetoresistance (AMR) behaviour were investigated.

2. Experimental

Figure 1 shows the fabrication process and the characterization of nanowires electrodeposited in a nanochannel: (a) heavy ion track formation, (b) track etching, (c) sputter-deposition of a gold layer on both film surfaces, the right one being reinforced by an additional copper layer and serving as cathode, and the left one as contact layer, (d) electrodeposition of nanowire, (e) nanowire in contact with the gold layer, (f) resistance measurement with external magnetic field. Polycarbonate films (thickness: 30 μm) were used as templates. First, by irradiation with a heavy-ion beam of the UNILAC linear accelerator at GSI (Darmstadt, Germany) straight ion tracks were created perpendicular to the foil surfaces, as shown in Figure 1(a). The track densities ranged from a

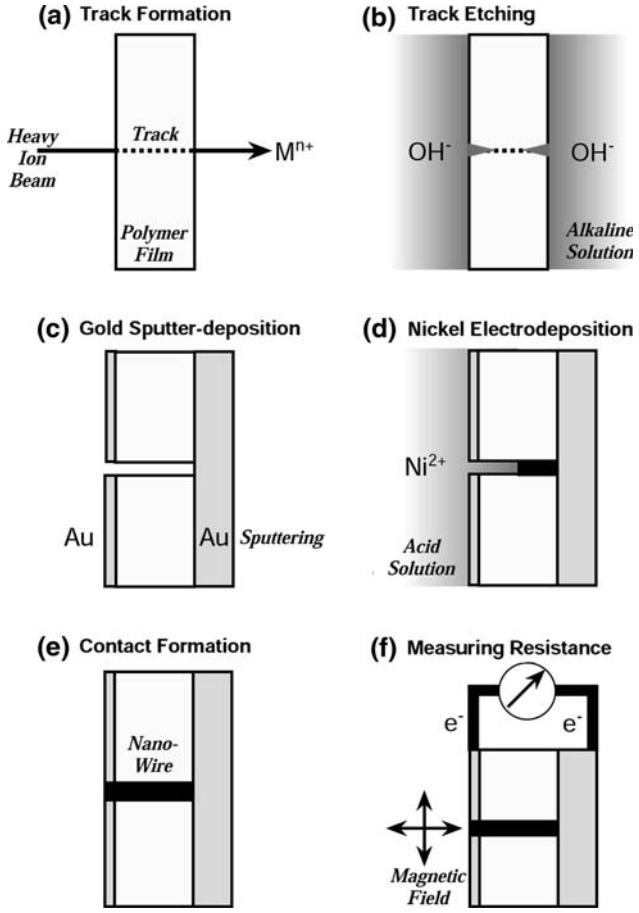

Fig. 1. Fabrication and characterization of a nanowire electrodeposited in a single-channel membrane. (a) track formation, (b) track etching in alkaline solution, (c) sputter-deposition of gold layers on both sides of the membrane, (d) electrodeposition of the wire, (e) contacting the growing wire with the metal layer on the opposite side, (f) measuring the wire resistance as function of an external magnetic field.

single track in a foil to 10^4 tracks cm^{-2}. Second, the tracks were selectively etched in an aqueous solution containing 6 mol l^{-1} sodium hydroxide to provide cylindrical nanochannels as shown in Figure 1(b). During etching, a constant voltage was applied between two electrodes separated by the film, and the current was used to monitor the etching process. The etching process was optimized to produce a uniform cross section along the channel with very small roughness. A gold layer of thickness 500 nm, later on used as cathode for nanowire growth, was sputter-deposited on one side of a nanoporous film, while a thin gold layer of thickness 100 nm, serving as contact layer for the nanowires, was placed on the other side as depicted in Figure 1(c). A gold wire with diameter of 1 mm was used as an anode. An aqueous electrolytic solution was synthesized from $NiSO_4 \cdot 7H_2O$ 120 g l^{-1} and H_3BO_3 45 g l^{-1}. The solution pH was 3.5 and the temperature was kept to 298 K. A cathodic polarization curve was drawn by plotting cathode potentials measured galvanostatically at each cathodic current to determine the optimum potential for nickel deposition. Nickel nanowires were electrodeposited potentiostatically at a cathode potential of -1.0 V vs. Ag/AgCl as shown in Figure 1(d). Growth rates were estimated by the channel filling time, which was determined from the time dependence of the deposition current. The wires contacted the gold layer when they reached the template surface (Figure 1(e)). Shape of nanowires was observed by using SEM (Philips XL 30 FEG). To obtain a SEM image of nanowires, polycarbonate template was removed by dichloromethane. The magnetoresistance of the wires was measured at room temperature applying a direct current of 10 μA and a magnetic field up to 10 kOe (Figure 1(f)).

3. Results and discussion

3.1. *Fabrication of nanochannels*

Figure 2 shows the time dependence of the current during etching of films with different track densities. The breakthrough times in Figure 2 are shifted to coincide at 300 s. In the time period before breakthrough (around 300 s), the current is extremely small due to the large resistance of the film. At breakthrough, the current increases drastically due to formation of open channels. The etching rate is estimated to be around 50 nm s^{-1} and does not depend on the density. After breakthrough, the current also increases due to the growing channel diameter.

The linear relationship between track density and current at various etching times is plotted in Figure 3. The channel diameter D_t (nm) at etching time t (s) can be estimated according to

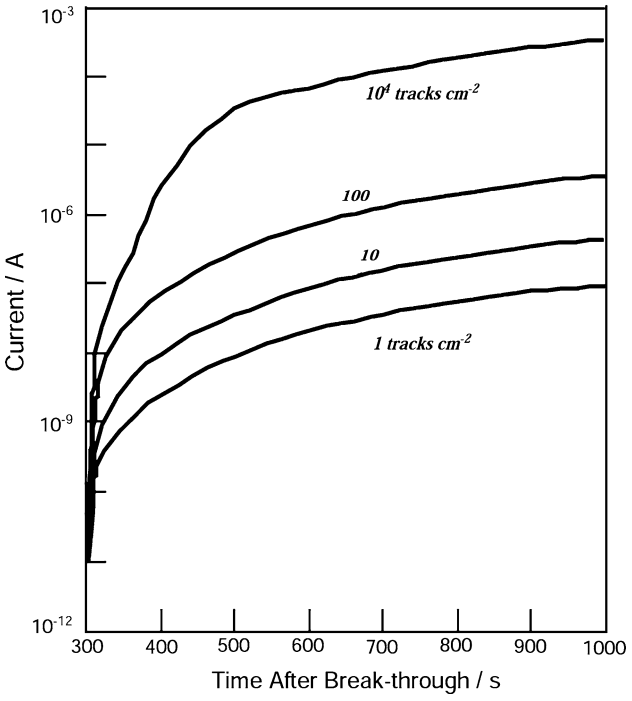

Fig. 2. Time dependence of current during track etching for samples with different heavy-ion-track densities (single-track membrane, 10, 100, and 10^4 tracks cm^{-2}).

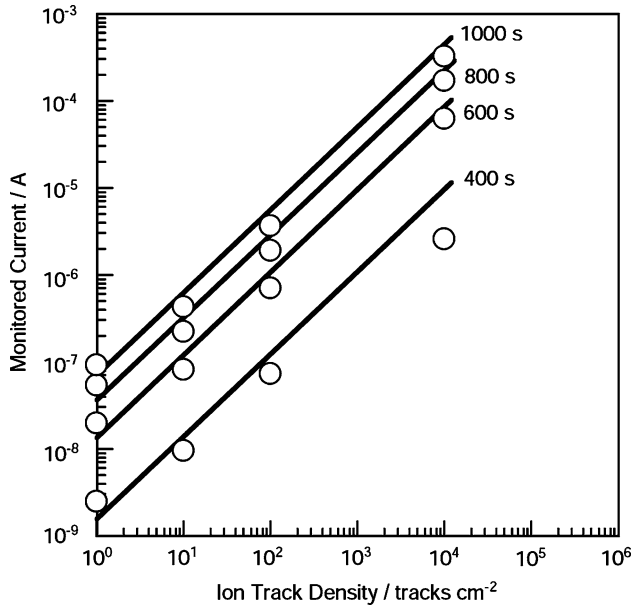

Fig. 3. Linear relationship between track density and current for etching times of 400, 600, 800, and 1000 s.

$$D_t = 2(\pi\sigma E)^{-0.5}(lI_e)^{0.5} = 10^{6.5}I_e^{0.5} \quad (1)$$

Here, E = voltage, I_e = current at etching time t, l = channel length, σ = conductivity of 6 M sodium hydroxide solution. In this study, $E = 1$ V, $l = 3 \times 10^4$ nm, and $\sigma = 0.04$ S cm^{-1}. At $t = 400$ s, I_e is around 10^{-9} A and D_{400} results in ~100 nm, whereas for $t = 1000$ s, I_e is about 10^{-7} A and D_{1000} amounts to ~1000 nm.

3.2. *Fabrication of nanowires*

The cathodic polarization curve of Figure 4 was recorded during electrodeposition of Ni^{2+} ions in a track-etched polycarbonate template with channel diameters of (500 ± 50) nm and an area density of 10^4 channels cm^{-2}. If the activity coefficient of Ni^{2+} ions, γ equals to 1, the equilibrium potential of Ni, E^{eq}, is estimated to be around −0.46 V vs. Ag/AgCl according to the following equation.

$$E^{eq} = E^0 + RT(nF)^{-1}\ln(\gamma C_{Ni}) \quad (2)$$

where, E^0 = standard electrode potential, C_{Ni} = concentration of Ni^{2+} ions. In this study, the electrolytic solution contains high concentration of Ni^{2+} ions. Therefore, γ is estimated to be less than 1 and E^{eq} would be less than −0.46 V. (For example, if γ is 0.1, E^{eq} is estimated to be around −0.49 V.) When a cathodic current of 10^{-5} A was applied to the nanochannel electrode, the cathode potential was around −0.1 V, which is nobler than the equilibrium potential of Ni and is close to that of hydrogen (ca. −0.2 V). This current corresponds to the hydrogen evolution. With increasing current, at ~10^{-5} A, the potential significantly polarizes from −0.4 to −0.7 V. This phenomenon seems to be caused by the concentration decrease of H^+ ions in the nanochannels. The consumption rate of H^+ in the channels increases with increasing cathodic current due to creation of molecular hydrogen, while the diffusion rate of H^+ from the bulk solution to the channels is independent of the current. Therefore, the H^+ concentration in the channels decreases with increasing current. At a potential less noble than the equilibrium potential of Ni, the current increases again at around −0.7 V. It is well known that iron-group metals such as Ni, Co, and Fe electrodeposit with an overpotential of approximately 0.2–0.3 V. Hence, this increase in cathodic current is mainly caused by an increase in the deposition current of Ni. At about 10^{-3} A, the potential significantly polarizes from −1.2 to −1.4 V. This phenomenon seems to be caused by the concentration decrease of Ni^{2+} ions in the channels. On the basis of the result given in Figure 4, the optimum deposition potential of Ni was determined to be ca. −1 V vs. Ag/AgCl.

Figure 5 visualizes the effect of channel density on time dependence of the cathodic current during electrodeposition of Ni^{2+} ions. Track-etched polycarbonate films with area densities from a single channel membrane to 10^4 channels cm^{-2} and channel diameters of (500 ± 50) nm were prepared as templates. During Ni^{2+} electrodepostion, the cathode potential was fixed at −1.0 V with respect to a Ag/AgCl reference electrode. In the case of a single-channel template, the cathodic current I_c was ~10^{-8} A over a time period of about 150 s. For each sample, the cathodic current rapidly increases after a deposition time of about 150 s. At this moment, the wires reach the membrane surface, and large hemispheric Ni caps start to form. The growth rate of Ni wires can be estimated to be ca. 200 nm s^{-1} by dividing the channel length ($l = 3 \times 10^4$ nm) by the filling time ($t = 150$ s).

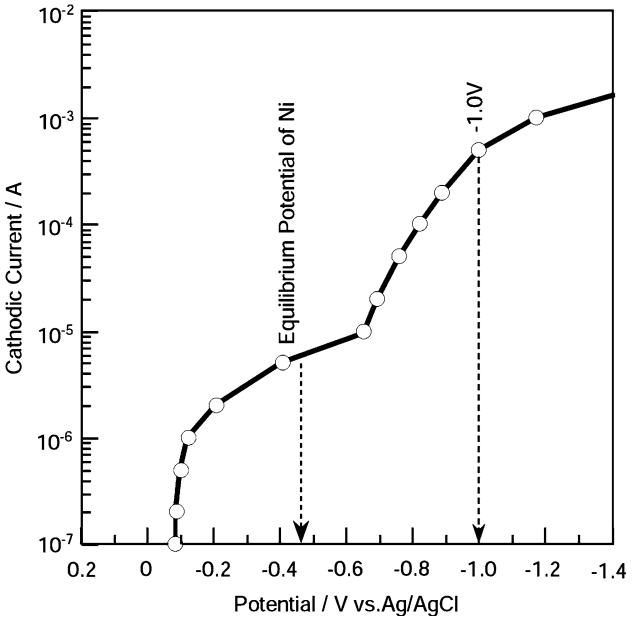

Fig. 4. Cathodic polarization curve of a heavy-ion-track etched polycarbonate template with a channel diameter (500 ± 50) nm and a density of 10^4 channels cm^{-2} in a solution containing Ni^{2+} ions.

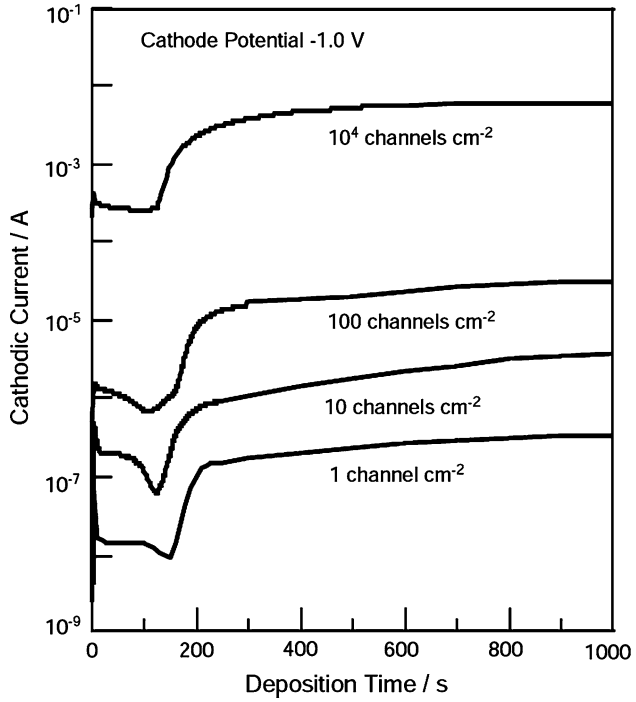

Fig. 5. Effect of channel density on cathodic current in a solution containing Ni^{2+} ions. Templates with channel diameter (500 ± 50) nm were used.

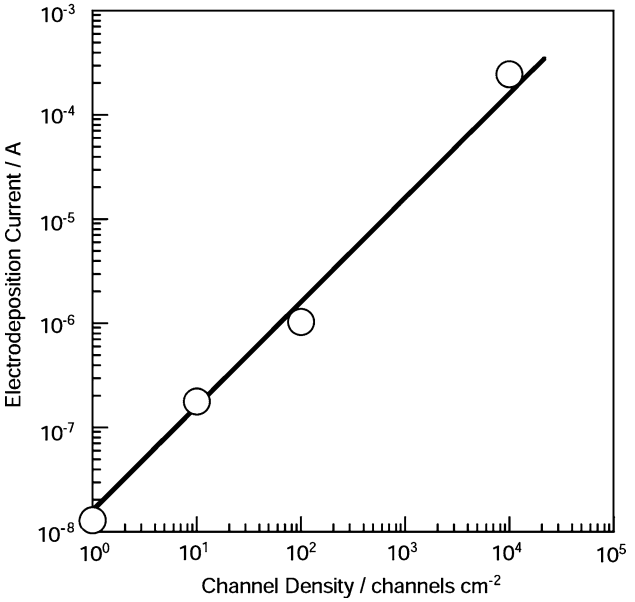

Fig. 6. Relationship between channel density and cathodic current for templates with a channel diameter (500 ± 50) nm, measured at a deposition time of 100 s.

The relationship between channel density and cathodic current recorded at a deposition time of 100 s is plotted in Figure 6. Templates with channel diameters (500 ± 50) nm were used for this measurement. With increasing channel density, the cathodic current increases linearly. The electrodeposition efficiency P (%) of Ni in etched-track templates can be estimated by

$$P = 25nF\pi D^2 l\rho(I_c t M_{Ni})^{-1} \quad (3)$$

Here, n = valence of Ni^{2+}, F = Faraday's constant, ρ = density of Ni deposit, I_c = cathodic current, and M_{Ni} = atomic weight of Ni. In this study, $n = 2$, $F = 96485$ C mol^{-1}, $\rho = 8.9$ g cm^{-3}, $M_{Ni} = 58.7$ g mol^{-1}. The electrodeposition efficiency P is estimated to roughly 10%.

3.3. *Characterization of nanochannels*

To obtain a SEM image of nanowires, a sample was prepared as follows. Firstly, Ni nanowires of length 10 μm were electrodeposited into a polycarbonate template of thickness 30 μm, channel diameter (500 ± 50) nm and area density 10^4 channel cm^{-2}. Then, the template was removed by an organic solvent. Finally, a thin gold layer of thickness 10 nm was sputter-deposited on the sample to avoid charging during SEM observation. Figure 7 shows a micrograph of Ni nanowires separated from the template. The average diameter corresponds well to that of the channels, and the cylindrical shape of the channels was perfectly transferred.

Homogeneous Ni nanowires and Co/Cu multi-layered nanowires electrodeposited in commercially available polycarbonate membrane filters are known to possess characteristic transport properties such as AMR and current-perpendicular-to-plane giant magnetoresistance (CPP-GMR) [3–5]. Figure 8 displays magnetoresistive hysteresis curves of a Ni nanowire in a single-channel template with a channel diameter of (500 ± 50) nm. Here, the MR ratio is defined by

$$\text{MR ratio}(\%) = 100(R_{max} - R_{min})R_{min}^{-1} \quad (4)$$

where, R_{max} and R_{min} are the resistance at zero and saturation field, respectively. The AMR curves exhibit the usual dependence on the direction of the applied magnetic field. In the direction parallel to the wire (0°), the effect of the magnetic field on the resistance is very small and the MR ratio is almost zero, while in the direction perpendicular to the wire (90°), the MR effect is maximum. An AMR ratio of 1.0% was observed for a Ni nanowire, which is typical of this system. Without magnetic field, the resistance of a Ni nanowire is around 198.2 Ω. Here, length and diameter of the nanowire are 30 μm and 500 nm. Therefore, the resistivity is estimated to be around 130 $\mu\Omega$ cm. This value confirms that the electrodeposited nanowire has metallic state [19].

Figure 9 displays the angular dependence of the normalized resistance measured at a magnetic field of 10 kOe for a Ni nanowire in a single-channel template with a channel diameter (500 ± 50) nm, θ being the angle between magnetic field and wire axis (= direction of current). The normalized resistance is well represented by a $\cos^2\theta$ curve. This result confirms that the track-etched polycarbonate film has straight channels perpendicular to its surface.

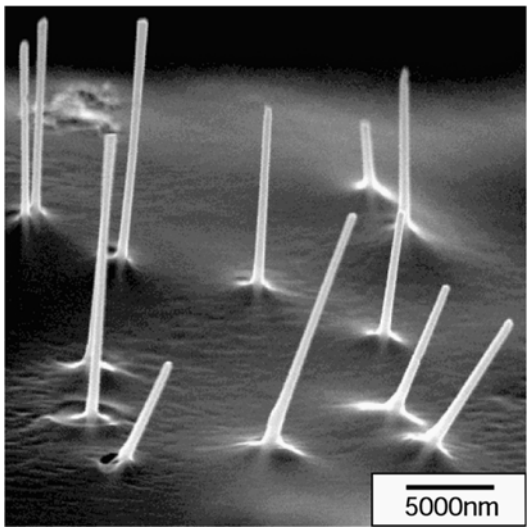

Fig. 7. SEM image of Ni nanowires with diameter (500 ± 50) nm and a channel density of 10^4 channel cm^{-2}.

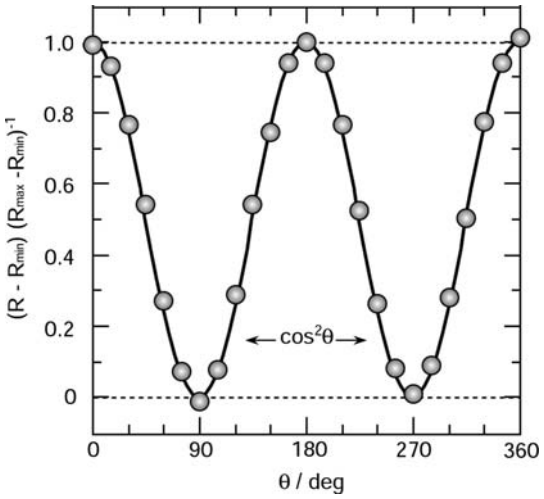

Fig. 9. Angular dependence of the normalized resistance measured at a magnetic field of 10 kOe of a single Ni nanowire of diameter (500 ± 50) nm.

4. Conclusion

Using energetic heavy ions, nanoporous polycarbonate templates with a wide range of channel densities were synthesized and Ni nanowires were electrodeposited in these templates. The technique can be employed to manufacture high-quality magnetic angle sensors based on the AMR effect. The track density and diameter can be controlled by ion fluence and etching time, respectively. Homogeneous Ni nanowires were successfully electrodeposited in these templates. The deposition efficiency was estimated to be around 10% at a deposition potential of −1 V using an Ag/AgCl reference electrode. The AMR of the wires reached 1%, sufficient for technical applications such as directional magnetic field sensors.

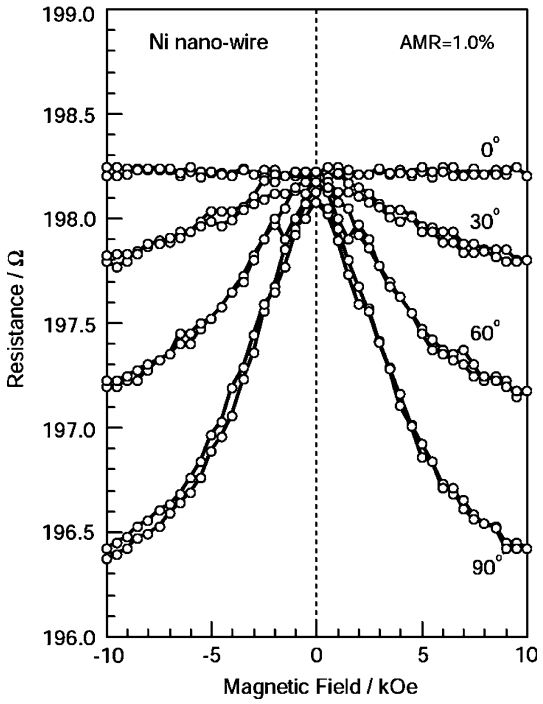

Fig. 8. Magnetoresistive curves of a Ni nanowire electrodeposited into a single-pore template with a channel diameter (500 ± 50) nm.

Acknowledgements

This work was supported in part by European Network on Ion Track Technology, EuNITT (HPRN-CT-2000-00047), Izumi Science & Technology Foundation (H16-J-139), Saneyoshi Scholarship Foundation (No. 1708), Mitutoyo Association for Science & Technology (MAST), Yazaki Memorial Foundation for Science & Technology and Japan Society for the Promotion of Science, Grant-in-aid for Young Scientists (B) (No. 17760581).

References

1. T.M. Whitney, J.S. Jiang, P.C. Searson and C.L. Chien, *Science* **261** (1993) 1316.
2. C.R. Martin, *Science* **266** (1994) 1961.
3. R. Ferre, K. Ounadjela, J.M. George, L. Piraux and S. Dubois, *Phys. Rev. B* **56** (1997) 14066.
4. J.E. Wegrowe, D. Kelly, A. Franck, S.E. Gilbert and J.-Ph. Ansermet, *Phys. Rev. Lett.* **82** (1999) 3681.
5. P.R. Evans, G. Yi and W. Schwarzacher, *Appl. Phys. Lett.* **76** (2000) 481.
6. D. Aimawlawi, N. Coombs and M. Moskovits, *J. Appl. Phys.* **70** (1991) 4421.
7. A. Tayaoka, E. Tayaoka and J. Yamasaki, *J. Appl. Phys.* **79** (1996) 6016.
8. F. Li and R.M. Metzger, *J. Appl. Phys.* **81** (1997) 3806.
9. P. Forrer, F. Schlottig, H. Siegenthaler and M. Textor, *J. Appl. Electrochem.* **30** (2002) 533.
10. K. Nielsch, F. Müller, A.P. Li and U. Gösele, *Adv. Mater.* **12** (2000) 582.
11. G. Sauer, G. Brehm, S. Schneider, K. Nielsch, R.B. Wehrspohn, J. Choi, H. Hofmeister and U. Gösele, *J. Appl. Phys.* **91** (2002) 3243.

12. T. Ohgai, X. Hoffer, L. Gravier, J.E. Wegrowe and J.-Ph. Ansermet, *Nanotechnology* **14** (2003) 978.
13. T. Ohgai, X. Hoffer, A. Fabian, L. Gravier and J.-Ph. Ansermet, *J. Mater. Chem.* **13** (2003) 2530.
14. M.E. Toimil-Molares, V. Buschmann, D. Dobrev, R. Neumann, R. Scholz, I.U. Schuchert and J. Vetter, *Adv. Mater.* **13** (2001) 62.
15. Z. Siwy, P. Apel, D. Baur, D. Dobrev, Y.E. Korchev, R. Neumann, R. Spohr, C. Trautmann and K. Voss, *Surface Sci.* **532–535** (2003) 1061.
16. I. Enculescu, Z. Siwy, D. Dobrev, C. Trautmann, M.E. Toimil Molares, R. Neumann, K. Hjort, L. Westerberg and R. Spohr, *Appl. Phys. A Mater. Sci. Process.* **77** (2003) 751.
17. N. Chtanko, M.E. Toimil Molares, T. Cornelius, D. Dobrev and R. Neumann, *J. Phys. Chem. B* **108** (2004) 9950.
18. D. Dobrev, D. Baur and R. Neumann, *Appl. Phys. A Mater. Sci. Process.* **80** (2005) 451.
19. T. Ohgai, L. Gravier, X. Hoffer, M. Lindeberg, K. Hjort, R. Spohr and J.-Ph. Ansermet, *J. Phys. D Appl. Phys.* **36** (2003) 3109.